J. Fluid Mech. (1976), *vol.* 77, *part* 4, *pp.* 685–708
Printed in Great Britain

On the spin-up and spin-down of a rotating fluid. Part 1. Extending the Wedemeyer model

By PATRICK D. WEIDMAN

Department of Aerospace Engineering, University of Southern California, Los Angeles

(Received 29 March 1974 and in revised form 27 March 1975)

The Wedemeyer model describing the spin-up of a fluid in a rotating cylinder is generalized to include the case of spin-down. Attention is focused on spin-up and spin-down at a finite (constant) acceleration for small Ekman numbers E_Ω. It is found that when the full nonlinear Ekman suction is included for spin-up from rest, the characteristics near the propagating wave front intersect, thus yielding an $O(1)$ velocity discontinuity for the inviscid model. This anomalous behaviour is limited to only a small range of Rossby numbers and does not appear in any of the spin-down solutions. Transient spin-down velocity profiles in the $O(E_\Omega^{\frac{1}{4}})$ shear layer at the cylindrical wall are calculated for the quasi-steady flow which occurs for sufficiently small decelerations. Results for impulsive spin-up and spin-down between infinite parallel plates are presented and compared with the asymptotic solutions given by Greenspan & Weinbaum and Benton. Finally, characteristic spin-up and spin-down times are computed for both the contained cylinder and the infinite-parallel-plates geometry.

1. Introduction

A revival in the study of the spin-up and spin-down of a rotating fluid has been motivated by the relatively recent paper of Greenspan & Howard (1963; hereafter denoted by G & H). They considered small, impulsive changes about a state of solid-body rotation of both a contained fluid and a fluid between infinite parallel plates; the initial angular velocity was Ω and the final angular velocity $\Omega(1+\epsilon)$, where ϵ is a Rossby number which measures the degree of nonlinearity. G & H have shown that the solution for the linearized problem ($\epsilon \ll 1$) for small Ekman number $E_\Omega = \nu/h^2\Omega$ gives a spin-up time scale $O(E_\Omega^{-\frac{1}{2}}\,\Omega^{-1})$, where h is the characteristic dimension along the axis of rotation and ν is the kinematic viscosity of the fluid. In this limit the spin-up time is much longer than the Ekman-layer formation time $O(\Omega^{-1})$ but considerably shorter than the time $O(E_\Omega^{-1}\,\Omega^{-1})$ for viscous diffusion, and hence the mechanism for spin-up of the interior fluid is one of vortex stretching. Also, the linearized analysis shows that the spin-up and spin-down times are equal.

Succeeding papers by Wedemeyer (1964), Greenspan & Weinbaum (1965) and Benton (1973) have provided results which, in one way or another, account for nonlinear effects. An excellent review of these and other studies of the spin-up problem is given by Benton & Clark (1974), and hence we shall not discuss them

in detail. Nevertheless, it is worthwhile to mention some important results. Greenspan & Weinbaum (to be denoted by G & W) included nonlinear effects by an expansion in terms of ϵ and presented solutions valid for moderate Rossby numbers. Benton (1973), using the method of matched asymptotic expansions, has presented solutions for the fully nonlinear problems of spin-up and spin-down between infinite parallel plates. However, his approximate analysis of the nonlinear Ekman flow must likewise limit these results to moderate Rossby numbers. The important conclusion drawn from both analyses is that the nonlinear interactions are small compared with the basic viscous processes and thus the spin-up time scale remains $O(E_\Omega^{-\frac{1}{2}}\,\Omega^{-1})$. Moreover, both investigations clearly demonstrate that nonlinear spin-down takes longer than nonlinear spin-up for the same effective Rossby number.

Motivation for the present investigation stemmed from the work of Wedemeyer (1964), who used a unique approximate method to formulate the hitherto unsolved problem of impulsive spin-up from rest of a contained fluid. Wedemeyer's work will be discussed in some detail in later sections since the assumptions inherent in his model apply to the present analysis as well. In essence, Wedemeyer has shown that spin-up in a cylinder is characterized by a cylindrical wave front (a discontinuity in shear) which propagates from the cylinder wall to the central axis. During this time the entire volume of fluid ahead of the wave front is eventually pumped through the Ekman layers and ejected into the region behind.

Many authors have since modified or extended Wedemeyer's model. Greenspan (1968), for example, has extended Wedemeyer's work to include spin-up from an arbitrary initial angular velocity for a general class of axially symmetric containers. Venezian (1969, 1970) has also adopted the Wedemeyer model and considered in detail the flow in the neighbourhood of the wave front for spin-up from rest. More recently, Watkins & Hussey (1973, 1976) have carried out the lengthy integrations of the full viscous Wedemeyer equation for several moderately small values of E_Ω. All of the above studies confirm that the spin-up time scale is still $O(E_\Omega^{-\frac{1}{2}}\,\Omega^{-1})$ for cylinder aspect ratios of order unity, thus corroborating G & W's conclusion that the nonlinear effects are indeed small.

The present investigation was initiated to offer a direct comparison between the predictions afforded by the Wedemeyer model (part 1) and experiment (part 2). Also, we consider the more general problem of finite angular acceleration, of which impulsive accelerations are a limiting case. In §2 a generalized form of Wedemeyer's equation is developed to include spin-down. Solutions for specific cases of spin-up and spin-down in a cylindrical container are given in §§3 and 4, respectively. In §5 we present results for impulsive spin-up and spin-down between infinite parallel plates and concluding remarks are given in §6.

2. The generalized Wedemeyer model

We shall use an inertial reference system whose origin is located at the centre of the cylinder. The natural co-ordinates are cylindrical (r, θ, z) and the respective velocity components will be denoted by (u, v, w). The vertical (z) axis is aligned along the geometric axis of the cylinder, which itself is coincident with the

rotation vector $\Omega\mathbf{k}$. The flat lids are located at $z = \pm\frac{1}{2}h$ and the cylindrical wall lies at $r = a$. We restrict ourselves to the case $E_\Omega \ll 1$, where $E_\Omega = \nu/\Omega h^2$ is the appropriately defined Ekman number. Since the Ekman-layer thickness δ is equal to $(\nu/\Omega)^{\frac{1}{2}}$, one concludes that $\delta/h \ll 1$ and consequently the horizontal boundary layers are confined to a thin region near the top and bottom lids.

The equation derived by Wedemeyer describing the axially symmetric incompressible fluid motion is

$$\frac{\partial v}{\partial t} + u\left(\frac{\partial v}{\partial r} + \frac{v}{r}\right) = \nu\left(\frac{\partial^2 v}{\partial r^2} + \frac{\partial}{\partial r}\left(\frac{v}{r}\right)\right). \tag{2.1}$$

The formal perturbation expansion in powers of $E_\Omega^{\frac{1}{2}}$ presented by Greenspan (1968, pp. 162–163) shows that the $O(1)$ motion satisfies the Taylor–Proudman theorem and, consequently, $v = v(r,t)$ only. It is then evident from (2.1) that $u = u(r,t)$ only, and, in particular, one would like to have an equation relating u and v to complete the problem formulation. An approximate relationship for spin-up was given by Wedemeyer; this approximation will now be generalized to include the case of spin-down.

Wedemeyer used the steady Ekman flux calculations of Rogers & Lance (1960) for fluid in solid-body rotation (ω) above an infinite rotating disk (Ω) to determine the local suction into the Ekman boundary layers for the unsteady problem of spin-up within an enclosed cylindrical container. Rogers & Lance (henceforth referred to as R & L) computed the nonlinear boundary-layer flow for eight values of $s = \omega/\Omega$ in the range $0 \leqslant s \leqslant 1$ and for eight values of $\sigma = \Omega/\omega$ in the range $0 \leqslant \sigma \leqslant 1$, thus covering the entire gamut of relative velocities from Kármán flow ($s = 0$) to Bödewadt flow ($\sigma = 0$). Their results for the Ekman suction can be expressed in the form

$$w_\infty(t) = \begin{cases} -\nu^{\frac{1}{2}}\Omega^{\frac{1}{2}} f(s), & \text{for} \quad 0 \leqslant s \leqslant 1, \\ -\nu^{\frac{1}{2}}\omega^{\frac{1}{2}} g(\sigma), & \text{for} \quad 0 \leqslant \sigma \leqslant 1, \end{cases} \tag{2.2}$$

where the functions $f(s)$ and $g(\sigma)$ are obtained by drawing a smooth curve through the computed points as indicated in figure 1. The blowing or suction $w_\infty(t)$ is written as a function of time since we now apply (2.2) to the unsteady flow problem. R & L's computations have been confirmed directly at one intermediate point in the range $0 < s < 1$ by Benton (1968). Furthermore, Carrier (1971) has obtained an approximate (implicit) formula for the Ekman suction which is in surprisingly close agreement with the calculations of R & L in the entire range $0 \leqslant \sigma \leqslant 1$. Thus there seems to be little doubt about the accuracy of their numerical calculations, in spite of the anomalous non-monotonic dependence of the Ekman suction on Rossby number near $s = 0$.

We make the following assumptions when applying R & L's results to spin-up or spin-down in a cylindrical container.

(i) The flow is quasi-steady.

(ii) The finite geometry does not affect the boundary-layer flux.

(iii) The fluid is locally in solid-body rotation.

The quasi-steady approximation (i) is adequate because, as pointed out by Benton (1973), time plays a passive role. Indeed, even in response to a nonlinear

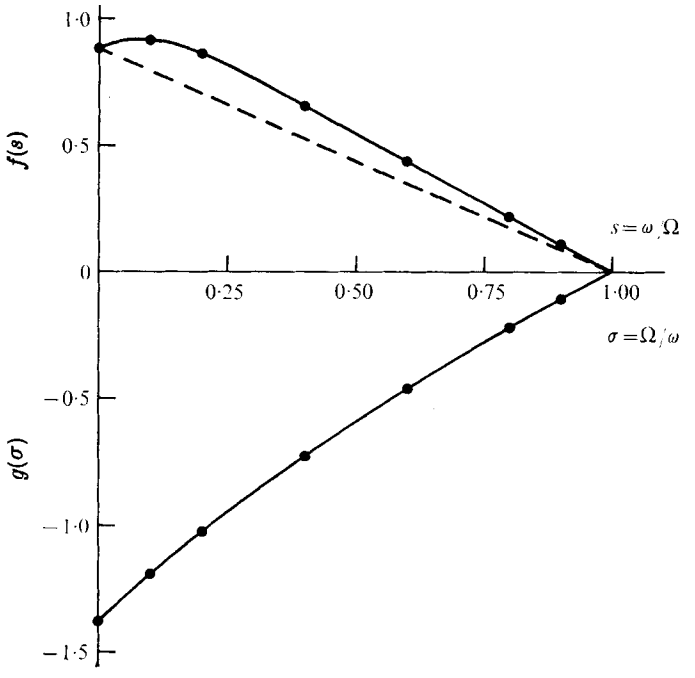

FIGURE 1. Ekman suction as a function of s (upper curve) and σ (lower curve). ●, calculations due to Rogers & Lance; ——, fitted curve; – – –, Wedemeyer's approximation.

change in wall speed, Benton (1966) has shown that the Ekman layers form in a time $O(\Omega^{-1})$. Thus on the spin-up time scale $O(E_\Omega^{-\frac{1}{2}}\Omega^{-1})$, the boundary-layer flow is steady in the limit $E_\Omega \to 0$. In (ii) we are assuming that, to leading order, the presence of the vertical walls does not alter the Ekman pumping. Linearized theories (cf. G & H; Stewartson 1957) indicate that the influence of a vertical wall or a split between differentially rotating disks is felt (directly) in a relatively narrow layer of thickness $O(E_\Omega^{\frac{1}{4}}h)$ at most. But the indirect influences are significant since they bring about cellular flow patterns which would not otherwise exist. We presume that qualitatively similar results will prevail in the nonlinear case. Perhaps assumption (iii) is the most restrictive; it is equivalent to saying that the mass flux along horizontal boundaries depends only on the local difference in vorticity across the Ekman layer. It may well depend on the gradients of axial vorticity when such gradients are large. In this event the interior flow would no longer be locally controlled by the Ekman layers.

Conservation of mass across a cylindrical sheet spanning the end plates requires

$$u(r, t) = (r/h)\, w_\infty(t), \tag{2.3}$$

and this in conjunction with (2.2) provides the desired relation $u = u(v)$. Combining these results gives the following nonlinear partial differential equations for the $O(1)$ interior fluid motion:

$$\frac{\partial v}{\partial t} - \frac{\nu^{\frac{1}{2}}}{h}\begin{Bmatrix}\Omega^{\frac{1}{2}}f(s)\\ \omega^{\frac{1}{2}}g(\sigma)\end{Bmatrix}\frac{\partial}{\partial r}(rv) = \nu\frac{\partial}{\partial r}\left(\frac{1}{r}\frac{\partial}{\partial r}(rv)\right). \tag{2.4}$$

n	a_n	b_n
0	0·88446	−1·36961
1	1·07258	1·81302
2	−9·44264	−0·83396
3	23·88193	1·86910
4	−38·45380	−4·31832
5	38·23662	5·41466
6	−21·06589	−3·47646
7	4·88674	0·90157

TABLE 1. Coefficients for the polynomial curve fits for $f(s)$ and $g(\sigma)$ according to (2.6)

For spin-up the expression $\Omega^{\frac{1}{2}}f(s)$ is used; this is the equation derived by Wedemeyer. For the case of spin-down the appropriate term is $\omega^{\frac{1}{2}}g(\sigma)$. The form of s and σ depends on the boundary conditions. For impulsive accelerations, s and σ will be functions of r and v alone, but in the event that the walls are accelerated at a finite rate, they will also be explicit functions of time. Solving (2.4) gives the interior azimuthal velocity and consequently u can be determined from (2.3). The axial velocity is then calculated from the equation of continuity

$$w(r,z,t) = -\frac{z}{r}\frac{\partial}{\partial r}(ru). \tag{2.5}$$

This 'integral method' effectively separates the details of the Ekman boundary layer from the geostrophic interior, linking them only by the suction which drives the flow. In other words, (2.2) provides us with a nonlinear Ekman compatability condition. Though some details of the fluid motion are lost (e.g. the inertial oscillations in the fluid interior), this approximate method has the capability of including the full nonlinear Ekman-layer behaviour in the limit $E_\Omega \to 0$.

2.1. *Curve fits of Rogers & Lance's data*

For the case of spin-up from rest, Wedemeyer further simplified the convection term in (2.4) by approximating the Ekman suction with the linear fit indicated in figure 1. This gives a maximum error of the order of 15 %.

In the present study we seek more accurate approximations for the curves $f(s)$ and $g(\sigma)$ in order to include the full nonlinear behaviour of the Ekman layers. Very accurate least-squares polynomial fits are given by

$$f(s) = \sum_{n=0}^{7} a_n s^n, \quad g(\sigma) = \sum_{n=0}^{7} b_n \sigma^n, \tag{2.6}$$

where $0 \leqslant s, \sigma \leqslant 1$, and the coefficients a_n and b_n are listed in table 1. The polynomial approximations have a standard deviation of less than 2×10^{-4} and are everywhere smooth and continuous.

In addition to these exact curve fits, simple analytic functions were sought which perhaps could lend themselves to useful closed-form solutions to the

differential equations. No such expression could be found for $f(s)$, but $g(\sigma)$ can be well approximated by a rational function. This expression, written in terms of $s = 1/\sigma$, is given by

$$g(s) = -K(s-1)/(s+b), \tag{2.7}$$

where $K = 1{\cdot}36961$ and $b = 0{\cdot}35300$. Equation (2.7) exactly satisfies the no-pumping condition at $s = 1$ as well as the Bödewadt blowing condition at $s = \infty$. At the intermediate points the approximate curve is everywhere within 0·8 % of R & L's calculations.

The approximations for $f(s)$ and $g(\sigma)$ cited above cover the entire range [0, 1] of the independent variables, a necessary condition when the initial or final state is one of quiescence. However, a linear approximation about $s = \sigma = 1$ will prove sufficient for some flows, even when there is a large difference between the initial and final rotational speeds. For example, if the cylinder is accelerated or decelerated at a slow enough rate, the local fluid velocity is expected not to lag far behind that of the wall and, consequently, the local Rossby number will remain small. In this case we shall appeal to the linear approximations

$$f(s) = k(1-s), \quad g(\sigma) = k(\sigma-1), \tag{2.8}$$

where the constant k is chosen to give the best fit over the range of interest. We note that $k = 1$ corresponds to linearized theory.

3. The problem of spin-up

It is convenient to begin with a discussion of impulsive spin-up and briefly present the results obtained from Wedemeyer's linear Ekman-suction approximation for later reference. We then show the effects of including the full nonlinear behaviour of the Ekman layer and proceed to the case of spin-up at constant acceleration. For the remainder of the presentation, variables with an asterisk represent dimensional quantities and those without an asterisk are the corresponding non-dimensional variables.

3.1. *Impulsive spin-up*

We assume the cylinder and fluid to be initially in a state of solid-body rotation Ω_i and the speed of the cylindrical container to be impulsively increased to Ω_f. Then $s = \omega^*/\Omega_f$ and the inviscid portion of (2.4) can be written as

$$\frac{\partial v^*}{\partial t^*} - \frac{\nu^{\frac{1}{2}}}{h}\Omega_f^{\frac{1}{2}} r^* f\left(\frac{v^*}{r^*\Omega_f}\right)\left(\frac{\partial v^*}{\partial r^*} + \frac{v^*}{r^*}\right) = 0. \tag{3.1}$$

The dimensional variables v^*, r^* and t^* are then normalized with the characteristic values $a\Omega_f$, a and Ω_f^{-1} respectively. In terms of the circulation $\Gamma^* = r^*v^*$, the non-dimensional form of (3.1) is

$$\frac{\partial \Gamma}{\partial t} - E_\Omega^{\frac{1}{2}} r f\left(\frac{\Gamma}{r^2}\right)\frac{\partial \Gamma}{\partial r} = 0, \tag{3.2}$$

with the corresponding boundary conditions

$$\Gamma(r,0) = r^2\gamma, \quad 0 \leqslant r \leqslant 1, \tag{3.3a}$$

$$\Gamma(1,t) = 1, \qquad t > 0, \tag{3.3b}$$

where $E_\Omega = \nu/h^2\Omega_f$ is the Ekman number and $\gamma = \Omega_i/\Omega_f$. Equation (3.2), which is in the standard form for solving by the method of characteristics, shows that the circulation is conserved along characteristic paths defined by

$$dr/dt = -E_\Omega^{\frac{1}{2}} rf(\Gamma_0/r^2), \tag{3.4}$$

where Γ_0 is the constant value of the circulation. The characteristics constitute an expansion fan centred on $r = 1$ and $t = 0$ with, since $f(s) \geqslant 0$ everywhere, their paths running towards decreasing r. In general the characteristics would have to be determined by numerical integration. However, if we assume $f(s) = k(1-s)$, the following closed-form solution is obtained (cf. Ingersoll & Venezian 1968 or Venezian 1969):

$$\Gamma(r,t) = \gamma r^2/(r_0(t))^2 \quad \text{in region I}, \quad r \leqslant r_0(t), \tag{3.5a}$$

$$\Gamma(r,t) = (r^2 - \exp(-2\beta_1 t))/(1-\exp(-2\beta_1 t)) \quad \text{in region II}, \quad r \geqslant r_0(t), \tag{3.5b}$$

where $\beta_1 = kE_\Omega^{\frac{1}{2}}$ and

$$r_0(t) = [\gamma + (1-\gamma)\exp(-2\beta_1 t)]^{\frac{1}{2}}. \tag{3.5c}$$

The dividing characteristic, which will also be referred to as the wave front, propagates from the cylindrical wall to the final radial position $(r_0)_f = \gamma^{\frac{1}{2}}$; if $\gamma = 0$ we have spin-up from rest and the front eventually converges on the axis of the cylinder. The fluid ahead of the wave front spins up like a solid body while conserving angular momentum, and, although the angular velocity is continuous across $r_0(t)$, its derivative is not. Consequently, the dividing characteristic supports a discontinuity in shear. The radial velocity is likewise continuous across the front, but the vertical velocity w is discontinuous and in fact changes sign there. A direct consequence is that the Ekman suction, while being convergent ahead of $r_0(t)$, is divergent in the region behind. Moreover, since it can be shown that $u = dr_0/dt$ at the dividing characteristic, the front is actually a contact surface. The boundary conditions for u and v are satisfied at $r = 1$, but the vertical velocity determined from (2.5) is discontinuous at the cylindrical boundary.

3.2. *Vertical boundary and free shear layers*

Retention of the $O(E_\Omega)$ viscous terms in the azimuthal momentum equation for impulsive spin-up gives

$$\frac{\partial\Gamma}{\partial t} - E_\Omega^{\frac{1}{2}} rf\left(\frac{\Gamma}{r^2}\right)\frac{\partial\Gamma}{\partial r} = A^2 E_\Omega\left[\frac{\partial^2\Gamma}{\partial r^2} - \frac{1}{r}\frac{\partial\Gamma}{\partial r}\right], \tag{3.6}$$

where $A = h/a$ is the cylinder aspect ratio. With a change of co-ordinates such that the wave front is located at a constant value of one of the independent variables, Venezian (1970) analysed the structure of the propagating free shear layer for the velocity profiles obtained by Wedemeyer. Under the assumption

$AE_\Omega^{\frac{1}{4}} \ll 1$, he was able to reduce (3.6) to the one-dimensional Burgers equation, the solution of which smooths out the shear discontinuity in a thickness $O(E_\Omega^{\frac{1}{4}}h)$. The transition layer grows with time owing to both convective and diffusive processes. All the velocities vary continuously through the shear layer and so an embedded inner layer is not required.

Consider now the flow near the cylindrical boundary. It is a simple matter to show that the full viscous equation for the linear approximation to $f(s)$ is satisfied by the inviscid solution (3.5*b*), since the bracketed term in (3.6) vanishes identically. Hence an $O(E_\Omega^{\frac{1}{4}})$ vertical boundary layer, generally required to smooth out $O(1)$ discontinuities in shear or velocity, does not appear, although an attached $O(E_\Omega^{\frac{1}{4}})$ layer is necessary in order to make the vertical velocity continuous at the wall. In the linear analysis of G & H, the double layers remain attached to the wall, but for the nonlinear case Venezian has shown that the $O(E_\Omega^{\frac{1}{4}})$ layer propagates away from the wall along the dividing characteristic $r_0(t)$. The conclusion is, therefore, that the nonlinearity separates the double structure of the vertical boundary layer.

3.3. *A closer look at the wave front*

In an attempt to obtain the 'exact' solution for the inviscid flow in the interior, the paths of the characteristic curves defined by (3.4) were determined numerically using (2.6) for the fully nonlinear Ekman suction. These calculations gave the unexpected result that the characteristics always intersected in the region of the wave front for spin-up from rest. It was eventually guessed that this behaviour was due to the non-monotonicity of the function $f(s)$. That this conjecture is in fact true can be seen from the following analysis.

Integration of (3.4) for an arbitrary (well-behaved) $f(s)$ satisfying the initial condition $r = 1$ at $t = 0$ gives

$$E_\Omega^{\frac{1}{2}} t = -\int_1^r \frac{dx}{xf(\Gamma_0/x^2)}.$$

With the change of variables $x^2\xi = \Gamma_0$, the characteristic curves satisfy the relation

$$H(r,t;\Gamma_0) = E_\Omega^{\frac{1}{2}} t - \int_{\Gamma_0}^{\Gamma_0/r^2} \frac{d\xi}{\xi f(\xi)} = 0, \tag{3.7}$$

and the envelope of intersecting characteristics, if it exists, is given by (see, for example, Courant 1936, pp. 172–173)

$$dH(r,t;\Gamma_0)/dt = 0.$$

Differentiation of (3.7) with the aid of Leibnitz's rule shows that this condition can be satisfied if

$$f(\Gamma_0) = f(\Gamma_0/r^2), \tag{3.8}$$

which is simply a statement of non-monotonicity. Since $0 \leqslant r \leqslant 1$ we must have $\Gamma_0/r^2 \geqslant \Gamma_0$ as depicted in figure 2. Actually, since $\gamma \leqslant \Gamma_0 \leqslant 1$, condition (3.8) will be satisfied only when $\gamma \leqslant s_1$, where s_1 is the position of the maximum Ekman suction. From the least-squares fit, $s_1 = 0{\cdot}075$ and $f(s_1) = 0{\cdot}921$. In particular, the characteristics will always intersect for spin-up from rest, and consequently

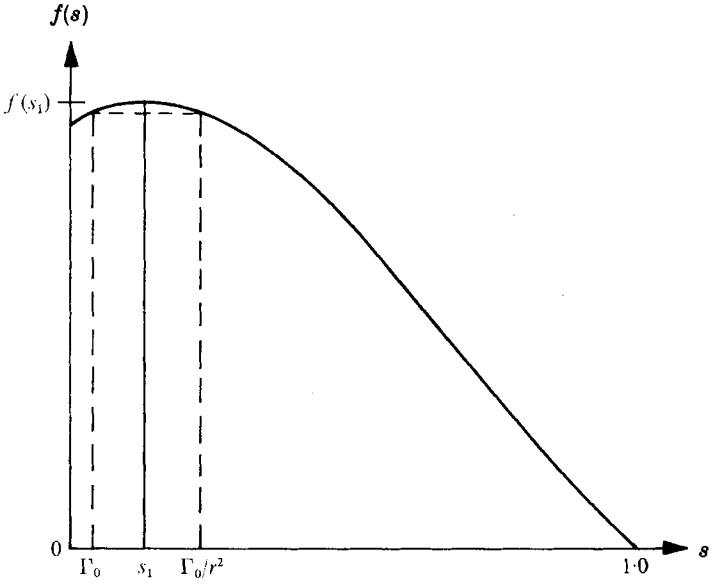

FIGURE 2. Sketch showing the values of s for which characteristic paths will intersect for impulsive spin-up. The maximum at $s_1 = 0{\cdot}075$ is $f(s_1) = 0{\cdot}921$.

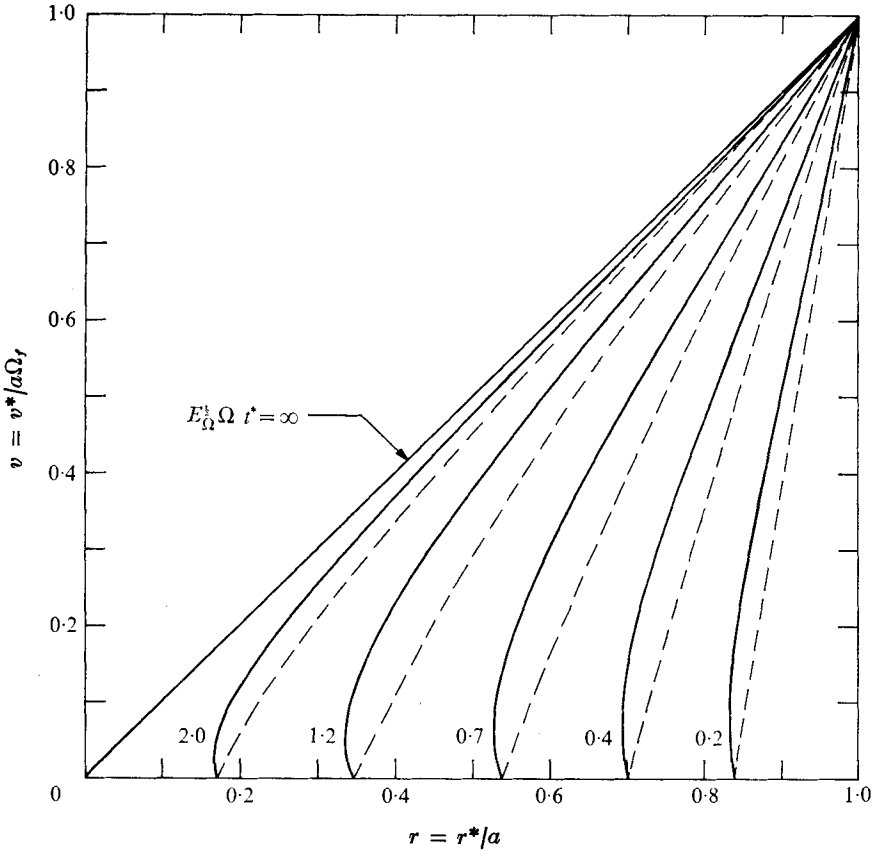

FIGURE 3. Velocity profiles for impulsive spin-up from rest of an inviscid fluid with $E_\Omega^{\frac{1}{2}}\Omega t^*$ as a parameter. ——, solution with exact fit to $f(s)$; – – –, Wedemeyer's solution.

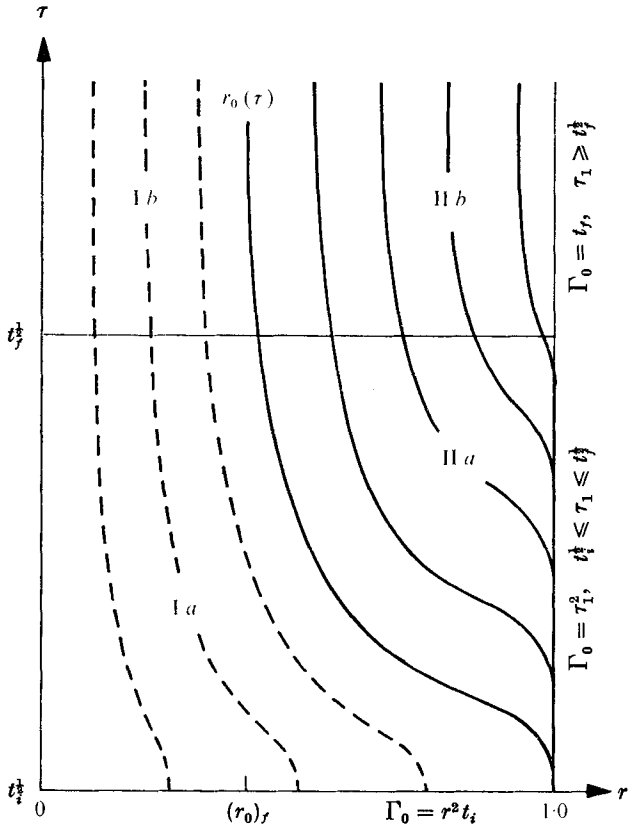

FIGURE 4. Characteristic paths and boundary values for spin-up at constant acceleration.

the wave front is characterized by a velocity discontinuity instead of the shear discontinuity predicted in Wedemeyer's approximate analysis.

Owing to this additional complication, the correct inviscid solution near the wave front becomes much more elusive. We shall postpone a discussion of this problem and simply present in figure 3 a typical set of velocity profiles for spin-up from rest, ignoring the correct behaviour near the wave front; the double-valued solution is a direct consequence of the non-monotonic Ekman flux curve used in the mathematical model. Also included in figure 3 are the results obtained by Wedemeyer for his linear approximation to $f(s)$.

3.4. *Spin-up at constant acceleration*

Now consider the case in which the cylinder is uniformly accelerated at a constant rate α between the initial and final angular velocities. During the acceleration phase $s = \omega^*/(\Omega_i + \alpha t^*)$, and normalizing the dimensional variables (cf. §3.1) with the characteristic quantities $\alpha^{\frac{1}{2}}a$, a and $\alpha^{-\frac{1}{2}}$, we arrive at the inviscid circulation equation

$$\frac{\partial \Gamma}{\partial \tau} - 2E_\alpha^{\frac{1}{2}} r\tau^2 f\left(\frac{\Gamma}{r^2\tau^2}\right)\frac{\partial \Gamma}{\partial r} = 0, \tag{3.9}$$

where $\tau = (t+t_i)^{\frac{1}{2}}$ is the transformed time and $t_i = \Omega_i/\alpha^{\frac{1}{2}}$. Here the Ekman number is defined as $E_\alpha = \nu/h^2\alpha^{\frac{1}{2}}$. The boundary conditions to be satisfied are

$$\Gamma(r, t_i^{\frac{1}{2}}) = r^2 t_i \quad \text{for} \quad 0 \leqslant r \leqslant 1, \tag{3.10a}$$

$$\Gamma(1, \tau) = \tau^2 \quad \text{for} \quad \tau \geqslant t_i^{\frac{1}{2}}. \tag{3.10b}$$

As in the impulsive case, the solution requires that the circulation remain constant (Γ_0) along characteristic paths now given by

$$dr/d\tau = -2E_\alpha^{\frac{1}{2}} r\tau^2 f(\Gamma_0/r^2\tau^2), \tag{3.11}$$

and again we see that all the curves run to the left. Boundary conditions and typical paths qualitatively corresponding to the linear approximation to $f(s)$ are sketched in figure 4. The horizontal line at $\tau = t_f^{\frac{1}{2}}$, where $t_f = \Omega_f/\alpha^{\frac{1}{2}}$, marks the end of the acceleration period and thus (3.9) describes the motion only in regions I a and II a. The characteristic paths are then extended into regions I b and II b with the aid of the impulsive spin-up equation, using the calculated solution along $\tau = t_f^{\frac{1}{2}}$ as initial conditions. Numerical integrations again revealed that the characteristics intersect for acceleration from rest in the fully nonlinear case. That this must always happen could not be proved analytically because the variables in (3.11) cannot be separated. The result seems reasonable, however, since the entire non-monotonic curve is necessary to describe spin-up from rest, regardless of the manner in which the boundaries are accelerated.

3.5. *Constant acceleration solution for the linear approximation to $f(s)$*

With the proper choice of k, the linear approximation for the Ekman suction can be made quite good, even for moderate Rossby numbers as large as $\epsilon = 1-s = 0{\cdot}8$. In this case, (3.9) can be written as

$$\frac{\partial \Gamma}{\partial \tau} - \beta_2 \left(\frac{r^2\tau^2 - \Gamma}{r}\right) \frac{\partial \Gamma}{\partial r} = 0, \tag{3.12}$$

where $\beta_2 = 2kE_\alpha^{\frac{1}{2}}$. In regions I a, b the boundary conditions allow separation of variables and explicit solutions are obtained in terms of a simple quadrature. This is not the case in regions II a, b, where the characteristic paths must first be determined. We shall simply present the solutions, which the reader can verify by direct substitution.

In region I a, $r \leqslant r_0(\tau)$,

$$\Gamma(r,\tau) = r^2 G(\tau) = \frac{t_i \exp(c\tau^3)\, r^2}{\exp(ct_i^3) + 3c^{\frac{2}{3}} t_i [I(c^{\frac{1}{3}}\tau) - I(c^{\frac{1}{3}} t_i^{\frac{1}{2}})]}, \tag{3.13}$$

and in region II a, $r \geqslant r_0(\tau)$,

$$\Gamma = \Gamma_0 = \tau_1^2, \quad t_i \leqslant \tau_1^2 \leqslant t_f, \tag{3.14a}$$

along the characteristics

$$r^2(\tau) = \exp(-c\tau^3)\,[\exp(-c\tau_1^3) + 3c^{\frac{2}{3}}\tau_1^2\{I(c^{\frac{1}{3}}\tau) - I(c^{\frac{1}{3}}\tau_1)\}]. \tag{3.14b}$$

In the above expressions, $c = \frac{2}{3}\beta_2$, and the integral is given by

$$I(x) = \int^x \exp(\xi^3)\, d\xi.$$

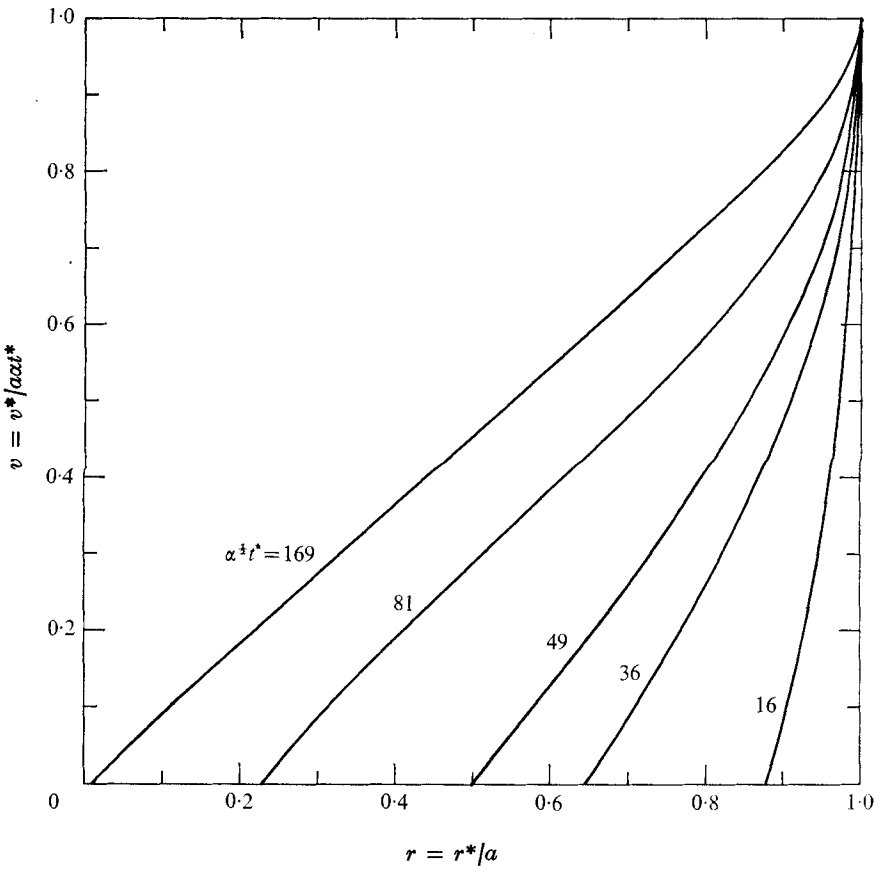

FIGURE 5. Velocity profiles for spin-up from rest at constant acceleration with $\alpha^{\frac{1}{2}}t^*$ as a parameter; $E_\alpha = 9{\cdot}82 \times 10^{-6}$.

The dividing characteristic $r_0(\tau)$ is found by setting $\tau_1 = t_i^{\frac{1}{2}}$ in (3.14). Once $I(x)$ is evaluated, the circulation at each position and time during the acceleration phase can be determined.

For the post-acceleration period the cylinder walls rotate at constant angular speed Ω_f and so $s = \omega^*/\Omega_f$. Thus we use (3.1) for impulsive spin-up, only now the non-dimensionalization is carried out with the same characteristic quantities as are used for non-dimensionalization in this section, namely $\alpha^{\frac{1}{2}}a$, a and $\alpha^{-\frac{1}{2}}$. The resulting equation for the linear approximation to $f(s)$ is then

$$\frac{\partial \Gamma}{\partial t} - \beta_3 \left(\frac{r^2 t_f - \Gamma}{r} \right) \frac{\partial \Gamma}{\partial r} = 0, \tag{3.15}$$

where $\beta_3 = kE_\alpha^{\frac{1}{2}}/t_f^{\frac{1}{2}}$. Denoting the initial time as $t_0 = t_f - t_i$, we obtain the initial conditions

$$\Gamma(r, t_0) = r^2 G(t_f^{\frac{1}{2}}) = r^2 g_0 \quad \text{for} \quad r_0(t) \leqslant r \leqslant 1,$$

$$\tau = \tau_1(\xi), \quad r = \xi \quad \text{along} \quad t = t_0 \quad \text{for} \quad 0 \leqslant r \leqslant r_0(t),$$

which are calculated from (3.13) and (3.14). With this notation the post-acceleration solution in region Ib, $r \leqslant r_0(t)$, is given by

$$\Gamma(r,t) = \frac{r^2 t_f g_0}{g_0 - (g_0 - t_f)\exp\{-2\beta_3 t_f^{\frac{1}{2}}(t-t_0)\}} \tag{3.16}$$

and in region IIb, $r \geqslant r_0(t)$ we have

$$\Gamma = \Gamma_0 = \tau_1^2, \quad t_i \leqslant \tau_1^2 \leqslant t_f, \tag{3.17a}$$

along the characteristics

$$r^2(t) = \frac{\tau_1^2(\xi)}{t_f} + \left(\xi^2 - \frac{\tau_1^2(\xi)}{t_f}\right)\exp\{-\tfrac{1}{2}\beta_3 t_f^{\frac{1}{2}}(t-t_0)\}. \tag{3.17b}$$

The dividing characteristic $r_0(t)$ carries the circulation $\tau_1^2 = t_i$ and its final radial position,

$$(r_0)_f = t_i/t_f = (\Omega_i/\Omega_f)^{\frac{1}{2}},$$

is found by letting $t \to \infty$ in (3.17b).

Typical velocity profiles during the acceleration period for spin-up from rest according to (3.14) are presented in figure 5. The full nonlinear solution gives qualitatively similar results, except that the velocity discontinuity appears in lieu of the shear discontinuity. Interestingly enough, figure 5 shows that the angular velocity of the interior fluid is continually catching up with the angular speed of the walls, even though the cylinder does not stop accelerating. We note that the general discussion concerning the vertical boundary and free shear layers for impulsive spin-up given in §3.2 applies equally well to spin-up at constant acceleration.

4. The problem of spin-down

We consider now the unsteady motion of a fluid spinning down from an initial state of solid-body rotation Ω_i. The model equation is (2.4) with the Ekman suction given by $\omega^* {}^{\frac{1}{2}} g(\sigma)$ since now $\omega^* > \Omega$. As will be shown presently, the full $O(1)$ solution necessitates a consideration of the viscous boundary layer at the cylindrical wall. Thus, in addition to the interior solutions, we obtain velocity profiles near the wall by integrating the full viscous equation for the special case of quasi-steady spin-down.

Since the rational-function curve fit (2.7) reproduces R & L's numerical computations so well, we shall not resort to the exact polynomial curve fit as determined by the method of least squares.

4.1. *Impulsive spin-down*

For impulsive spin-down to the final angular velocity Ω_f, we have $s = \omega^*/\Omega_f$. Inserting (2.7) into (2.4) and normalizing v^*, r^* and t^* with $\Omega_i a$, a and Ω_i^{-1} respectively, one obtains the inviscid equation of motion

$$\frac{\partial \Gamma}{\partial t} + \beta_4 \left(\frac{\Gamma - \mu r^2}{\Gamma + b\mu r^2}\right)\frac{\partial \Gamma}{\partial r} = 0, \tag{4.1}$$

with $\mu = \Omega_f/\Omega_i$ and $\beta_4 = KE_\Omega^{\frac{1}{2}}$, where $E_\Omega = \nu/h^2\Omega_i$. The boundary conditions are

$$\Gamma(r,0) = r^2, \quad 0 \leqslant r \leqslant 1, \tag{4.2a}$$

$$\Gamma(1,t) = \mu, \quad t > 0. \tag{4.2b}$$

Now, since $g(\sigma) \leqslant 0$ everywhere, the characteristic curves for (4.1) all run towards increasing r. In particular, the vertical shear layer identified with the dividing characteristic emanating from $r = 1$ tries to propagate outside the cylindrical boundary, but since this is physically impossible it remains attached there. A second consequence is that the entire body of fluid in the cylinder remains in region I, and one can always find a solution of the form $\Gamma(r,t) = r^2F^2(t)$ as long as the initial condition is one of solid-body rotation. Inserting this product into (4.1) gives

$$\frac{dF}{dt} + \beta_4 F^2\left(\frac{F^2-\mu}{F^2+b\mu}\right) = 0, \tag{4.3}$$

with (4.2a) providing $F(0) = 1$. The integration is readily performed with the aid of partial fractions, however the solution,

$$t = \frac{1}{\beta_4}\left[b\frac{F-1}{F} + \frac{1+b}{2\mu^{\frac{1}{2}}}\ln\left(\frac{1-\mu^{\frac{1}{2}}}{1+\mu^{\frac{1}{2}}}\frac{F+\mu^{\frac{1}{2}}}{F-\mu^{\frac{1}{2}}}\right)\right], \tag{4.4}$$

can only be expressed as an implicit function of time. As expected, the boundary condition $F = \mu^{\frac{1}{2}}$ at the wall cannot be satisfied and thus we anticipate an $O(E_\Omega^{\frac{1}{4}})$ vertical shear layer. An explicit solution for spin-down to rest is obtained by taking the limit of (4.4) as $\mu \to 0$. In this case the circulation

$$\Gamma(r,t) = r^2/(1+\beta_4 t)^2 \quad (\mu = 0) \tag{4.5}$$

is seen to approach its final state algebraically, rather than exponentially as in (4.4).

The solution for the linear approximation to $g(\sigma)$ is included in (4.4) above, but we now set $b = 0$, replace the constant K with k according to (2.8), and write $\beta_4' = kE_\Omega^{\frac{1}{4}}$. With this simplification the circulation can be written explicitly as

$$\Gamma(r,t) = \mu\left[\frac{1+\mu^{\frac{1}{2}}+(1-\mu^{\frac{1}{2}})\exp(-2B_4'\mu^{\frac{1}{2}}t)}{1+\mu^{\frac{1}{2}}-(1-\mu^{\frac{1}{2}})\exp(-2\beta_4'\mu^{\frac{1}{2}}t)}\right]^2 r^2. \tag{4.6}$$

This impulsive spin-down solution for the linear approximation to $g(\sigma)$ looks quite different from the impulsive spin-up solution (3.5a) for the linear approximation to $f(s)$. However, in the limiting case $\epsilon = (1-\mu) = (1-\gamma) \to 0$, both solutions reduce to the linearized (long time) result given by G & H, provided we set $k = 1$.

4.2. *Spin-down at constant deceleration*

When the cylinder is decelerated at a constant rate we have $s = \omega^*/(\Omega_i - \alpha t^*)$, where α is the rate of deceleration. Scaling the variables with $\alpha^{\frac{1}{2}}a$, a and $\alpha^{-\frac{1}{2}}$, we obtain the dimensionless equation of motion

$$\frac{\partial\Gamma}{\partial\tau} - \beta_5\Gamma^{\frac{1}{2}}\left(\frac{\Gamma-\tau r^2}{\Gamma+b\tau r^2}\right)\frac{\partial\Gamma}{\partial r} = 0, \tag{4.7}$$

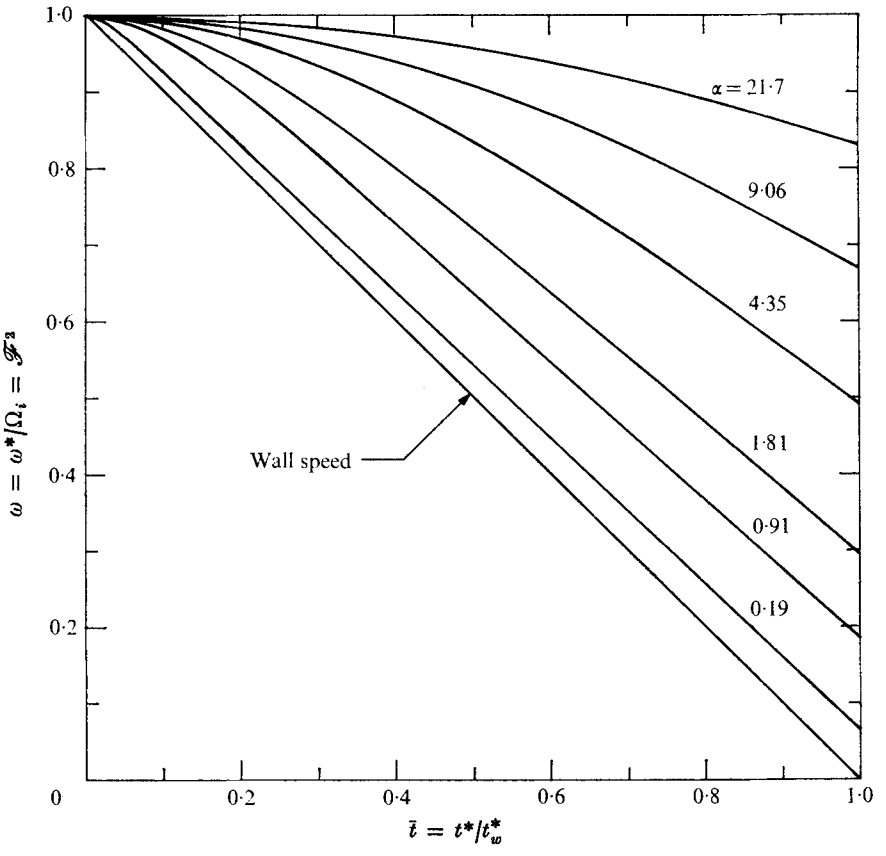

FIGURE 6. Angular velocity *vs.* time for spin-down at constant deceleration with α (rad/s^2) as a parameter; $\Omega_i = 109$ rad/s, $E_\Omega = 9{\cdot}27 \times 10^{-8}$.

with the associated boundary conditions

$$\Gamma(r, t_i) = r^2 t_i, \quad 0 \leqslant r \leqslant 1, \tag{4.8a}$$

$$\Gamma(1, \tau) = \tau, \qquad t_i \geqslant \tau \geqslant 0, \tag{4.8b}$$

where $\tau = t_i - t$ is the shifted time and $\beta_5 = KE_\alpha^{\frac{1}{2}}$. Both E_α and t_i retain the definitions given in § 3.4. We separate variables by writing $\Gamma(r, \tau) = r^2 \mathscr{F}^2(\tau)$ and obtain the ordinary differential equation

$$\frac{d\mathscr{F}}{d\tau} - \beta_5 \mathscr{F}^2 \left(\frac{\mathscr{F}^2 - \tau}{\mathscr{F}^2 + b\tau} \right) = 0, \tag{4.9}$$

where $\mathscr{F}$ must satisfy the initial condition $\mathscr{F}(t_i) = t_i^{\frac{1}{2}}$.

Although no closed-form solution of (4.9) could be found, a more fortunate circumstance prevails when $g(\sigma)$ is linear. In this case we set $b = 0$ in (4.9) and obtain the Ricatti-type equation

$$d\mathscr{F}/d\tau - \beta_6(\mathscr{F}^2 - \tau) = 0, \tag{4.10}$$

where now $\beta_6 = kE_\alpha^{\frac{1}{2}}$ in accordance with (2.8). With appropriate transformations

(4.10) can be reduced to the linear Airy equation, and the resulting solution for the circulation is

$$\Gamma(r,\tau) = \frac{1}{\beta_6^{\frac{2}{3}}}\left[\frac{\mathrm{Ai}'(\beta_6^{\frac{2}{3}}\tau)+k_0\,\mathrm{Bi}'(\beta_6^{\frac{2}{3}}\tau)}{\mathrm{Ai}(\beta_6^{\frac{2}{3}}\tau)+k_0\,\mathrm{Bi}(\beta_6^{\frac{2}{3}}\tau)}\right]^2 r^2, \tag{4.11}$$

where

$$k_0 = -\left[\frac{\mathrm{Ai}'(x_0)+x_0^{\frac{1}{2}}\,\mathrm{Ai}(x_0)}{\mathrm{Bi}'(x_0)+x_0^{\frac{1}{2}}\,\mathrm{Bi}(x_0)}\right], \quad x_0 = \beta_6^{\frac{2}{3}} t_i.$$

Ai and Bi are the tabulated (cf. Abramowitz & Stegun 1965, pp. 475–478) Airy functions of the first and second kind, respectively. In the above a prime denotes differentiation with respect to the argument.

Numerical solutions of the full nonlinear equation (4.9) showing the effect of the deceleration rate are presented in figure 6. Here time is non-dimensionalized by $t_w^* = \Omega_i/\alpha$, which is the time it takes for the cylinder walls to come to rest. The circulation determined by numerical integration of (4.9) or from (4.11) is, of course, valid only until the cylinder reaches its final steady speed Ω_f, where $\Omega_i > \Omega_f \geqslant 0$. The approach of the fluid motion to the final state is given by the impulsive spin-down solution. If the angular velocity of the fluid determined at the end of the deceleration period is denoted by Ω_0, then the post-deceleration solution is given by (4.4) or (4.6) with Ω_i everywhere replaced by Ω_0.

4.3. *Boundary layer at the cylindrical wall*

Although all velocity components in the inviscid solutions for spin-down are discontinuous at the cylindrical boundary, the only $O(1)$ discontinuity is in the azimuthal velocity. We expect a boundary-layer thickness $O(E_\Omega^{\frac{1}{2}})$ and, as this is many times larger than the Ekman-layer thickness, we assume that the local approximation for the Ekman suction is still valid. Hence the $O(1)$ circulation in the boundary layer should be adequately described by the full viscous equation (2.4).

It is well known (cf. Briley & Walls 1971) that for $E_\Omega \ll 1$ the fluid particles near the cylindrical wall will rapidly experience a centrifugal instability for finite amplitude impulsive spin-down. If the cylinder spins down over a finite period of time, one would expect the onset of the instability to be delayed, and in the limit of very slow deceleration the flow may never become unstable. With this motivation, it seems worthwhile to solve for the $O(1)$ velocity in the boundary layer for these 'quasi-steady' flows.

We begin the analysis by writing the full viscous equation of motion (2.4) in terms of the local angular velocity $\omega^* = v^*/r^*$. Following the development in §4.2, one obtains the non-dimensional equation

$$\frac{\partial\omega}{\partial\tau} - \beta_5\omega\left(\frac{\omega-\tau}{\omega+b\tau}\right)\left(r\frac{\partial\omega}{\partial r}+2\omega\right) = -A^2E_\alpha\left(\frac{\partial^2\omega}{\partial r^2}+\frac{3}{r}\frac{\partial\omega}{\partial r}\right), \tag{4.12}$$

and the angular velocity in the boundary layer must match up with the interior flow as well as satisfy the no-slip condition at the wall. These conditions are written as

$$\omega(r,\tau)\to\omega_I(\tau) = \mathscr{F}^2(\tau), \quad d\omega/dr(r,\tau)\to 0, \tag{4.13}$$

at the interior, and $\omega(1,\tau) = \tau, \quad t_i \geqslant \tau \geqslant 0,$

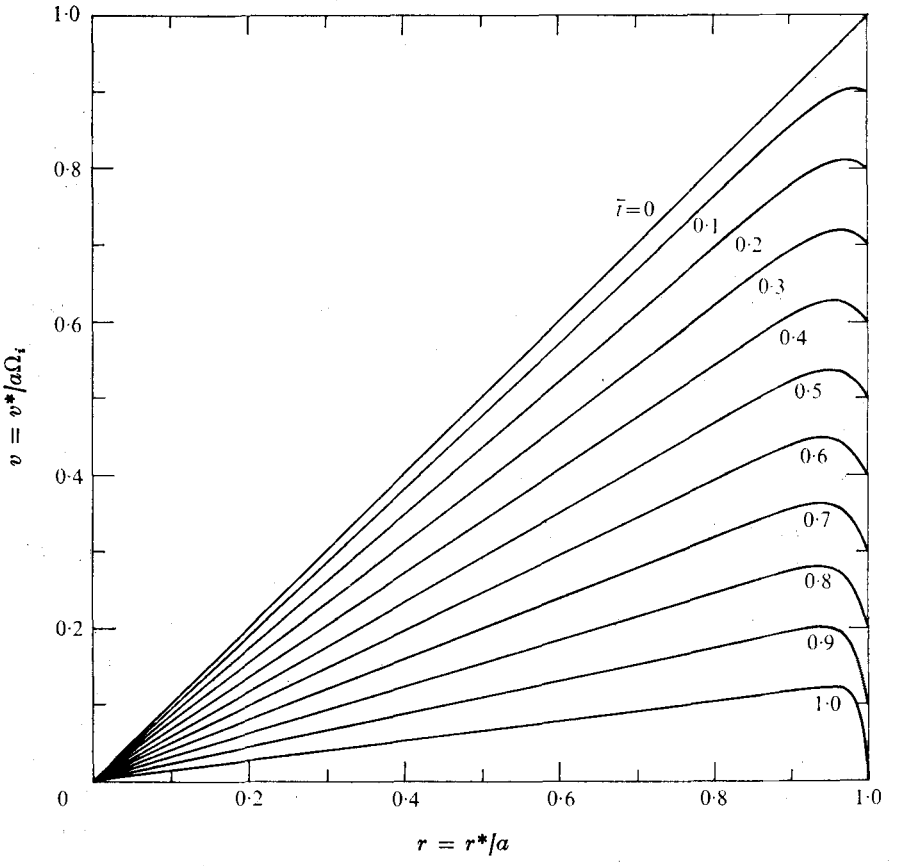

FIGURE 7. Velocity profiles for spin-down at constant deceleration with $\bar{t} = t^*/t^*_w$ as a parameter; $\Omega_i = 109$ rad/s, $E_\alpha = 13{\cdot}8 \times 10^{-6}$.

where $\mathscr{F}(\tau)$ satisfies (4.9) for the interior (subscript I) fluid motion. We proceed by scaling the dependent variable in a manner appropriate to a boundary-layer analysis, namely

$$\omega_B(r,\tau) = \frac{\omega-\omega_{\text{wall}}}{\omega_I-\omega_{\text{wall}}} = \frac{\omega-\tau}{\omega_I-\tau} = \frac{\omega-\tau}{\phi(\tau)}, \tag{4.14}$$

and the subscript B denotes 'boundary layer'. The unsteady term in (4.12) written in terms of the boundary-layer variable becomes

$$\partial\omega/\partial\tau = 1+\phi'\omega_B+\phi\omega'_B, \tag{4.15}$$

and here the prime represents partial differentiation with respect to τ. From the definition (4.14) we see that ω_B is constant in time, both at the wall and in the fluid interior, hence $\omega'_B = 0$ at these end points. We assume that the local fluid acceleration lies between its value at the wall and at the fluid interior, hence

$$\omega'_I \leqslant \omega' \leqslant 1. \tag{4.16}$$

The interior solutions displayed in figure 6 show that for sufficiently slow deceleration rates (in this case $\alpha \lesssim 0{\cdot}9\,\text{rad/s}^2$) $\omega'_I \simeq 1$ during the major portion of the

spin-down time ($t^*/t_w^* \gtrsim 0{\cdot}1$). From (4.16) we also obtain $\omega' \simeq 1$, and thus both the non-constant terms in (4.15) are small compared with one. We note that, whereas both $\phi\omega_B'$ and $\phi'\omega_B$ vanish at the wall, the former returns to zero in the interior while the latter approaches $\omega_I' - 1 \neq 0$; of these two small terms we choose to neglect $\phi\omega_B'$ in order to make the side-wall problem tractable and then use the experimental results to check the theory. In this approximation the fluid acceleration varies linearly with ω between its correct values at the end points, and the neglected term is then a correction to this linear dependence. Experiments (to be presented in part 2) indicate that this approximation is good at higher deceleration rates and even during the initial stage of spin-down, but there seems to be no easy way to ascertain this result *a priori*. In the limit of impulsive spin-down, however, this linear dependence cannot hold since the fluid acceleration approaches infinity.

Adopting the approximation described above, we find that (4.12) takes the form of an ordinary differential equation:

$$A^2 E_\alpha \left(\frac{d^2\omega}{dr^2} + \frac{3}{r}\frac{d\omega}{dr}\right) = \beta_5 \omega^{\frac{1}{2}} \left(r\frac{d\omega}{dr} + 2\omega\right)\left(\frac{\omega - \tau_1}{\omega + b\tau_1}\right) - \frac{\phi'(\tau_1)}{\phi(\tau_1)}(\omega - \tau_1) - 1, \quad (4.17)$$

where τ has been replaced by τ_1 to exemplify the fact that the flow is quasi-steady. Details of the numerical integration technique used to match the solution of (4.17) with the interior flow are given in the thesis of Weidman (1973). In figure 7 we present some velocity profiles for selected times $\bar{t} = t^*/t_w^*$ during the deceleration period. The numerical results show that the boundary layer (based on $\omega - \tau_1 = 0{\cdot}99(\omega_I - \tau_1)$) grows rapidly by diffusion to a thickness of order $hE_\Omega^{\frac{1}{4}}$, where Ω_i is used to calculate the Ekman number. The side-wall layer reaches a maximum near $\bar{t} = 0{\cdot}15$ and then gradually decreases to about half its peak value when the cylinder comes to rest. The radial velocity computed from (2.3) is continuous throughout the vertical shear layer, but the axial velocity remains discontinuous at $r = 1$.

5. Impulsive spin-up and spin-down between infinite parallel plates

The Wedemeyer approach is actually best suited to solving the problem of nonlinear spin-up and spin-down between infinite parallel plates. For this geometry we can immediately dispense with assumption (ii) in §2. Moreover, the von Kármán radial dependence for infinite parallel plates ensures that assumption (iii) will always be satisfied. Finally, in the limiting case $E_\Omega \to 0$, the quasi-steady approximation (i) is exact.

We use the same scaling of variables as in §§3.1 and 4.1 for impulsive spin-up and spin-down. After separating the radial dependence, we find the general solutions

$$\tau = 2E_\Omega^{\frac{1}{2}}\,\Omega_f t^* = \int_r^\omega \frac{dx}{xf(x)} \quad \text{(spin-up)}, \quad (5.1)$$

$$\tau = 2E_\Omega^{\frac{1}{2}}\,\Omega_i t^* = \int_1^\omega \frac{dx}{x^{\frac{3}{2}} g(\mu/x)} \quad \text{(spin-down)}. \quad (5.2)$$

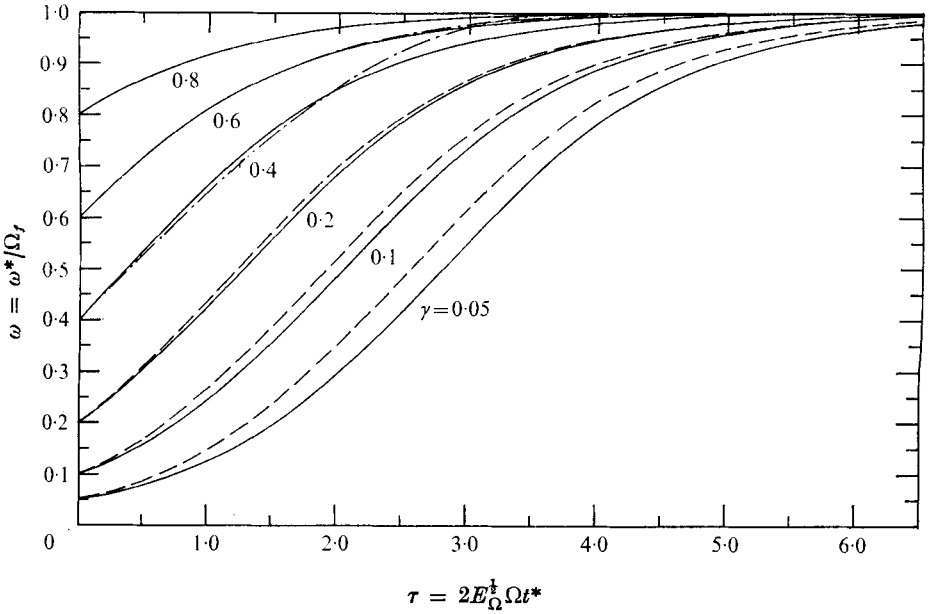

FIGURE 8. Angular velocity *vs.* time for impulsive spin-up between infinite parallel disks with $\gamma = \Omega_i/\Omega_f$ as a parameter. ——, present calculations; – – –, results due to Benton; —·—, results due to Greenspan & Weinbaum (plotted only down to $\gamma = 0{\cdot}4$).

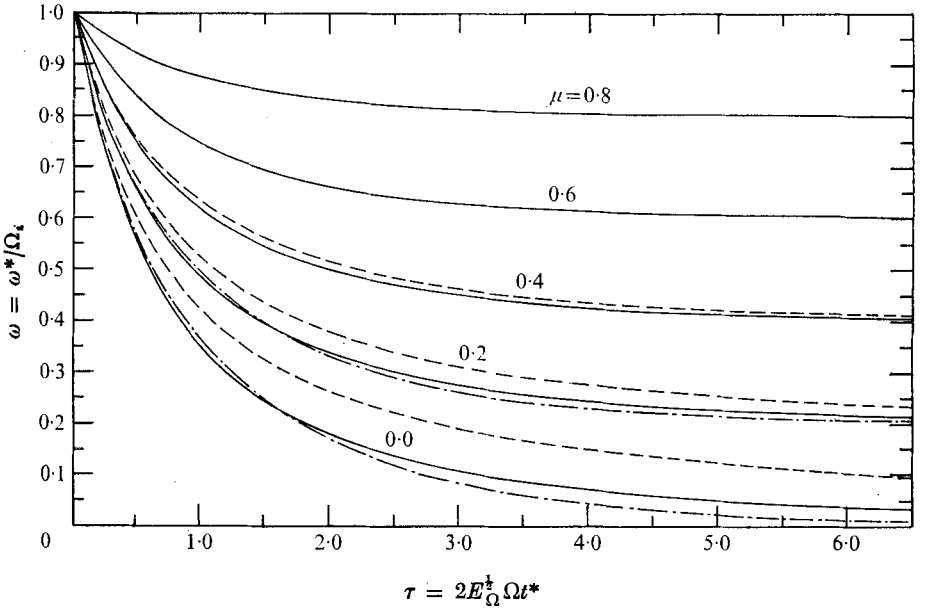

FIGURE 9. Angular velocity *vs.* time for impulsive spin-down between infinite parallel disks with $\mu = \Omega_f/\Omega_i$ as a parameter. ——, present calculations; – – –, results due to Benton; —·—, results due to Greenspan & Weinbaum.

The non-dimensional time τ has been chosen to be identical to that used by G & W and Benton (1973) in order to facilitate a comparison of results. Equations (5.1) and (5.2) were integrated for various values of γ and μ respectively. The polynomial expressions (2.6) were used in the integrations since they represent the best possible fits to R & L's data, although the closed-form solution (4.4) gives almost identical results for impulsive spin-down. The solution curves are given in figures 8 and 9 along with the results of G & W and Benton (1973).

Although Greenspan & Weinbaum state that their theory should be limited to moderate Rossby numbers, we see from figure 9 that they provide a reasonable approximation at larger Rossby numbers in the case of spin-down. Their solution for spin-up, however, does diverge rapidly for $\gamma < 0{\cdot}4$, and in fact becomes non-uniform in time. In Benton's analysis, the effects of the nonlinear Ekman layer are accounted for by a regular perturbation expansion in Rossby number truncated after the quadratic term (an approximation introduced to treat exactly the more interesting effects of inertial and electromagnetic nonlinearities in MHD spin-up). This explains why his solution gives shorter spin-up times and longer spin-down times than those given here for the full nonlinear problem. His perturbation expansion correctly predicts the positive curvature $f''(s)$ for the Ekman suction at $s = 1$ (cf. figure 1), but the true curvature continuously decreases on either side of this point. Consequently, the perturbation expansion overestimates the suction as $s \to 0$ and underestimates it as $s \to \infty$. Nevertheless, Benton's solution does point out the tendency towards algebraic decay for spin-down to rest, although the true decay rate $\omega \sim (1 + \frac{1}{2}K\tau)^{-2}$ is considerably faster than his asymptotic solution $\omega \sim (1 + \frac{3}{2}\tau)^{-1}$ predicts.

6. Discussion and conclusion

We have found that the inviscid solution for the fully nonlinear equation for spin-up proposed by Wedemeyer results in an intersection of the characteristics describing the wave front for the small range of initial velocities

$$0 < \Omega_i/\Omega_f < 0{\cdot}075.$$

This phenomena is due to the non-monotonic dependence of the Ekman suction on Rossby number and gives rise to an $O(1)$ discontinuity in the azimuthal velocity. An analytic description of this sharp velocity transition layer based on the present model would require a determination of appropriate 'jump' conditions and then, in order to determine the position and strength of the discontinuity, it is evident one would have to employ a shock-fitting technique similar to that used in compressible gasdynamics. This procedure would entail a great deal of work, perhaps without adding significantly to the physical understanding of the problem already given by Venezian (1970). Nevertheless, other than integrating the full viscous partial differential equation as did Watkins & Hussey (1976), this seems to be the only way to determine the speed of the wave front for this small parameter range.

Alternatively, as one of the reviewers of this paper has pointed out, the prediction of a shock may signify a breakdown of the inviscid Wedemeyer model;

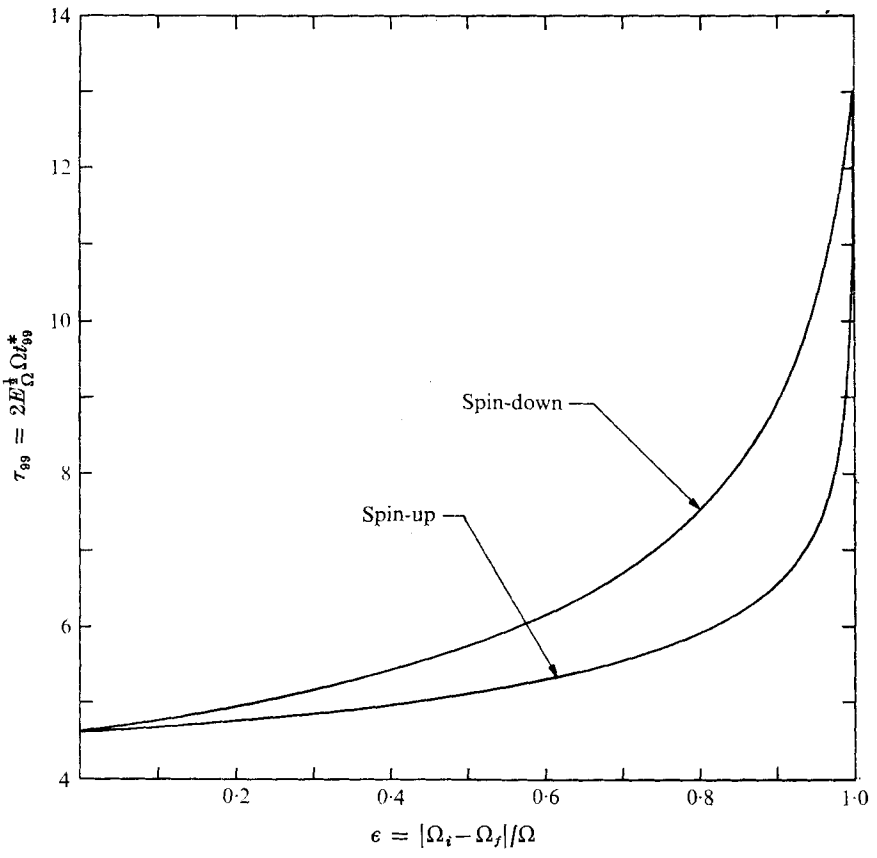

FIGURE 10. Characteristic times for spin-up and spin-down between infinite parallel disks as a function of Rossby number.

discontinuous radial gradients violate assumption (iii) in § 2, and hence the quasi-steady pumping given by Rogers & Lance's data would no longer be appropriate. In spite of the problems associated with the inviscid model, the calculations due to Watkins & Hussey (1973, 1976) show that any discontinuity which may exist is removed when the viscous terms in Wedemeyer's equation are included. The experiments presented in part 2 also show that the flow in the neighbourhood of the wave front takes the form of a viscous tongue which protrudes ahead of the convective velocity profile. This is consistent with Venezian's (1970) analysis, which suggests that discontinuities predicted by inviscid theory would be viscously smoothed in an $O(E_\Omega^{\frac{1}{4}})$ transition layer whose thickness varies with time and position. The existence or absence of a velocity discontinuity based on an *inviscid* analysis, however, remains an open question for further study.

Despite these uncertainties, it is tempting to consider the analogy between the spin-up of an incompressible fluid in a cylinder and the dynamics of a compressible gas, already noted by Benton & Clark (1974). Whereas the strength of a normal shock is given by the pressure jump $|\Delta P|/P_\infty$, the strength of the wave front for impulsive spin-up is given by the Rossby number $\epsilon = |\Delta\Omega|/\Omega_f$. Small Rossby

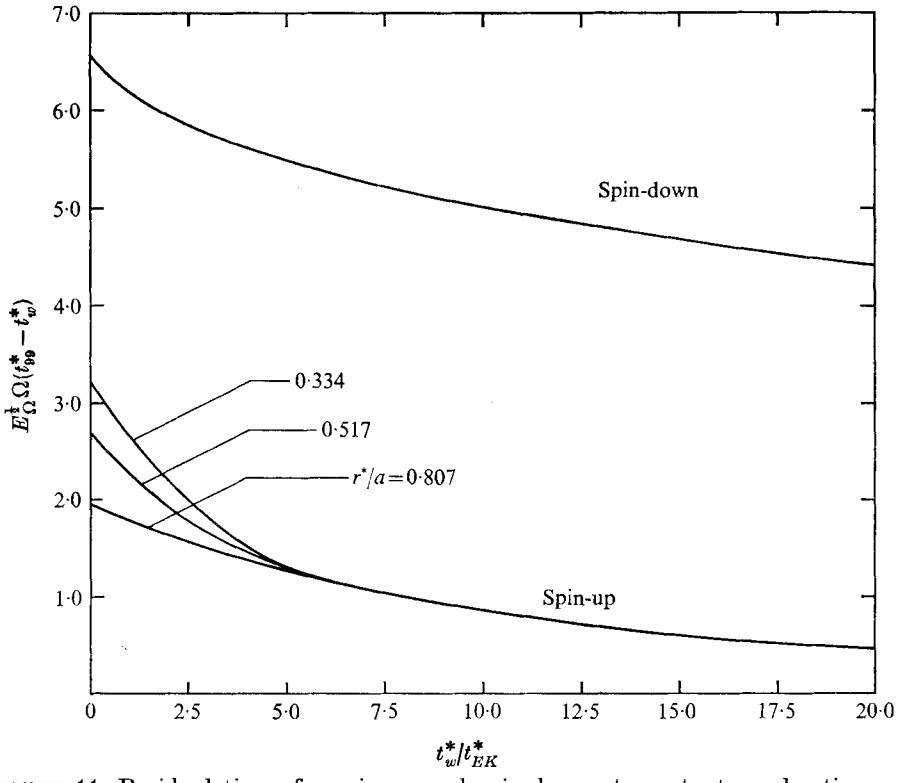

FIGURE 11. Residual times for spin-up and spin-down at constant acceleration *vs.* the acceleration time of the cylindrical container for $\epsilon = 1$; $\Omega = 109$ rad/s, $E_\Omega = 9{\cdot}27 \times 10^{-8}$.

number flows have 'weak' fronts of simply a shear discontinuity. In fact, Venezian (1970) has shown that the Burgers equation for compressible flow through a weak normal shock also describes the viscous structure of the weak front for spin-up. The shear front steepens with increasing ϵ and possibly develops into the higher-order velocity discontinuity for $\epsilon > 0{\cdot}925$. If this be the case, then these high Rossby number flows would be characterized by a 'strong' wave front according to the inviscid analysis.

Of practical interest is the time it takes for the bulk of the fluid to spin-up or spin-down. We designate t_{99}^* as the elapsed time for which the fluid locally reaches 99 % of the change in angular velocity imposed on the boundaries. In other words, the spin-up or spin-down time is defined as

$$\omega^*(t_{99}^*) = 0{\cdot}99\,|\Omega_i - \Omega_f|. \tag{6.1}$$

For the case of infinite parallel plates, the impulsive spin-up and spin-down times are radially independent. In figure 10 we present the characteristic times calculated from (5.1) and (5.2) as a function of the Rossby number $\epsilon = |\Omega_i - \Omega_f|/\Omega$, where $\Omega = \max(\Omega_i, \Omega_f)$. These curves confirm the results of G & W and Benton (1973); i.e., the nonlinearity increases the spin-up and spin-down times and nonlinear spin-up is achieved faster than nonlinear spin-down. The obvious exception near $\epsilon = 1$, where the spin-up time rapidly approaches infinity, is due to the

singular behaviour of (5.1) as $\gamma \to 0$. Physically, this corresponds to the fact that the interior motion is inviscid and conserves angular momentum, so spin-up from rest cannot take place since the initial angular momentum is everywhere zero.

The results in figure 10 also apply to impulsive spin-up and spin-down in an enclosed circular cylinder (in the limit $E_\Omega \to 0$) if we redefine the characteristic time t^*_{99} to be that for which *every* fluid particle has attained 99 % of the change in angular speed of the boundaries. The spin-up time according to (6.1), however, has a strong radial dependence. In figure 11 we display the effect of this radial dependence as well as the influence of the acceleration rate for the single case $\epsilon = 1$. The residual time $t^*_{99} - t^*_w$ for spin-up and spin-down in the ordinate is plotted against the period of acceleration or deceleration t^*_w normalized by $t^*_{EK} = E_\Omega^{-\frac{1}{2}} \Omega^{-1}$, the ordinary impulsive time scale. Again $\Omega = \max(\Omega_i, \Omega_f)$ and the nonlinear expressions (2.6) and (2.7) were used for $f(s)$ and $g(s)$ in the computations. This presentation presumes that the (unknown) detailed behaviour near the wave front will not significantly affect the global spin-up time.

The large difference between the results for spin-up and spin-down in figure 11 is due to the slow algebraic decay the fluid must always experience for spin-down to rest. Obviously, the presence of the cylindrical wall plays a dominant role when $\epsilon = 1$; fluid between infinite parallel plates does not spin-up from rest, but figure 11 shows that the bulk of the fluid in a bounded cylinder spins up even more rapidly than it spins down. We note that for $t^*_w/t^*_{EK} \ll 1$ the radial dependence indicative of impulsive spin-up obtains, but when $t^*_w/t^*_{EK} \gtrsim 5$ the influence of the propagating wave front is already forgotten and the approach to steady state is nearly that of solid-body spin-up. The transition between these two types of flows evidently occurs in the neighbourhood $t^*_w/t^*_{EK} = O(1)$. As $\alpha \to 0$ the residual spin-up and spin-down times also tend to zero, so in this limit $t^*_{99} \to t^*_w$.

The author wishes to acknowledge his mentor, Dr Tony Maxworthy, for many useful discussions of the spin-up problem. Thanks are also extended to Dr F. K. Browand, Dr B. A. Troesch, and Dr R. H. Edwards for their assistance and encouragement. The author is also grateful to Dr L. Redekopp, who read the manuscript and offered many valuable suggestions. This work was supported by the National Science Foundation under grant GK 19107.

REFERENCES

Abramowitz, M. & Stegun, A. 1965 *Handbook of Mathematical Functions*. Dover.

Benton, E. R. 1966 On the flow due to a rotating disk. *J. Fluid Mech.* **4**, 781–800.

Benton, E. R. 1968 A composite Ekman layer problem. *Tellus*, **20**, 667–672.

Benton, E. R. 1973 Nonlinear hydrodynamic and hydromagnetic spin-up driven by Ekman–Hartmann boundary layers. *J. Fluid Mech.* **57**, 337–360.

Benton, E. R. & Clark, A. 1974 *Ann. Rev. Fluid Mech.* **6**, 257–280.

Briley, W. R. & Walls, H. A. 1971 A numerical study of time dependent rotating flows in a cylindrical container at low and moderate Reynolds numbers. In *Proc. 2nd Int. Conf. Numerical Methods in Fluid Dyn., Berkeley*, pp. 377–384. Springer.

Carrier, G. F. 1971 Swirling flow boundary layers. *J. Fluid Mech.* **49**, 133–144.

Courant, R. 1936 *Differential and Integral Calculus*, vol. 2. Interscience.

GREENSPAN, H. P. 1968 *The Theory of Rotating Fluids*. Cambridge University Press.

GREENSPAN, H. P. & HOWARD, L. N. 1963 On a time dependent motion of a rotating fluid. *J. Fluid Mech.* **17**, 385–404.

GREENSPAN, H. P. & WEINBAUM, S. 1965 On nonlinear spin-up of a rotating fluid. *J. Fluid Mech.* **44**, 66–85.

INGERSOLL, A. P. & VENEZIAN, G. 1968 Nonlinear spin-up of a contained fluid. *Dept. Geolog. Sci., Calif. Inst. Tech., Pasadena, Contribution* no. 1612.

ROGERS, M. H. & LANCE, G. N. 1960 The rotationally symmetric flow of a viscous fluid in the presence of an infinite rotating disk. *J. Fluid Mech.* **7**, 617–631.

STEWARTSON, K. 1957 On almost rigid rotations. *J. Fluid Mech.* **3**, 17–26.

VENEZIAN, G. 1969 Spin up of a contained fluid. *Topics in Ocean Engng*, **1**, 212–223.

VENEZIAN, G. 1970 Non-linear spin-up. *Topics in Ocean Engng*, **2**, 87–96.

WATKINS, W. B. & HUSSEY, R. G. 1973 Spin-up from rest: limitations of the Wedemeyer model. *Phys. Fluids*, **16**, 1530–1531.

WATKINS, W. B. & HUSSEY, R. G. 1976 Spin-up from rest in a cylinder. *Phys. Fluids* (in press).

WEDEMEYER, E. H. 1964 The unsteady flow within a spinning cylinder. *J. Fluid Mech.* **20**, 383–399.

WEIDMAN, P. D. 1973 On the spin-up and spin-down of a contained fluid. Ph.D. thesis, Dept. Aerospace Engineering, University of Southern California, Los Angeles.